iMEDiTEC 2017

ORIGINAL PAPER

Shape Memory Alloy-based Actuator for Endoscopic Surgical Instrument

M. R. Abdul Kadir [a], D. E. O. Dewi [b,c,*], M. S. Mohamed Ali [d]

[a] Faculty of Biosciences and Medical Engineering, Universiti Teknologi Malaysia, 81310, Johor, Malaysia
[b] IJN-UTM Cardiovascular Engineering Center, Institute of Human Centered Engineering, Universiti Teknologi Malaysia, 81310, Johor, Malaysia
[c] Department of Clinical Science, Faculty of Biosciences and Medical Engineering, Universiti Teknologi Malaysia, 81310, Johor, Malaysia
[d] Faculty of Electrical Engineering, Universiti Teknologi Malaysia, 81310, Johor, Malaysia

* Corresponding author: dyah@utm.my

ABSTRACT

Highly flexible endoscopic instruments for Minimally Invasive Surgery play a vital role in performing a small insertion and surgical manoeuvre through narrow tubular space. This study was aimed to design, fabricate, test and analyse an instrument that functions as endoscopic tool with flexibility features. The study consisted of concept design, fabrication and testing methodologies. The design was made with 3D printing. Shape Memory Alloy was trained to bend into certain shapes. A silicone rubber sheathe was fabricated to act as a heat buffer. Bending and heat tests using thermal camera resulted in positive bending of about 30° consistently while the instrument was equipped without silicone rubber sheathe. Temperature readings on the thermal camera are 40°C. With the silicone rubber sheathe, the bending angle is halved over the entire instrument, but with a smaller decrease in recorded temperature of the spacer rings.

INTRODUCTION

Open surgery has been the mainstay of surgeons that makes large incision and instruments insertion to treat diseases or trauma openly (Park *et al.*, 2011). Open surgery recovery takes a longer time to recover and as such add more to the recovery cost. Minimally Invasive Surgery (MIS) has been considered as an alternative towards standard open surgery to reduce damages to surrounding tissues (Axcrona *et al.*, 2014). This operation only involves a small perforation in external tissue, thus entering the body through the small incision in the surrounding skin and muscle tissues. Although tissue damages can be reduced, the procedure limits the surgeon's capability to assess the internal tissue directly due to limited visibility and limited space of operation (Hansen *et al.*, 2010).

Endoscope, one of MIS instruments, has been widely used to reach the internal body area, observe, and manipulate the targeted tissue by cutting, drilling, or grasping the areas of interest, either for surgery, biopsy, treat, or cauterize any infected wounds (Hansen *et al.*, 2010). Currently, endoscope has been equipped with electrosurgical unit to enable for a more automatic insertion and maneuver (Vincent *et al.*, 2010). However, a rigid endoscope in the MIS can limit the flexibility and capabilities of the surgeon. To solve these, some endoscopic instruments are equipped with actuators to bend the instruments to reach the areas of interest or allow the surgeon to perform surgical procedures more easily (Haga *et al.*, 2005).

Nitinol has been commonly used as actuator, not only due to its high weight to force ratio, inertness and corrosion resistance, but also its shape memory property, so that it can change its shape if heat is applied to it (Vincent *et al.*, 2010). A Power Width Modulation(PWM) circuit is used as electrical heating of Nitinol to distribute the heat evenly along the actuator.

A surgical robot used Nitinol strip to develop a flexible endoscopic instrument by actuating a snake like robot in cranial MIS in tandem with Magnetic Resonance Imaging. It utilized a Power Width Modulator PWM switching circuit to control the Nitinol actuator. The

instrument consisted of a brass body connected by mechanical fixtures. Each segment had ±30° bending angle using antagonistic Nitinol strips (Bodner *et al.*, 2005). Yet, miniaturization became a problem as the brass body required mechanical fixture to bend with 2 degrees of freedom of each segment.

This study was aimed to overcome the issue of limited flexibility by designing and fabricating a new bending system for endoscopes with large angle bending using Shape Memory Alloy. This study consisted of concept design, fabrication and testing of the instrument though bend testing and observation through thermal camera.

MATERIALS AND METHODS

Design

The design consisted of the super-elastic backbone to push the instrument back to its original shape once the bending ended, the nitinol actuator which supplied the force for bending and the spacer rings which separated the actuators from preventing any unwanted activation of any adjacent actuator due to heat conduction.

The 3D printer material used Visijet FTX Green (Microsla, 3D Systems, Inc, North America). Super elastic alloy with a diameter of 0.49mm was used as the backbone of the instrument, an M type Nitinol alloy with a transformation temperature of 40°C and diameter of 0.49mm. The silicone rubber sheathe was fabricated using Shin Etsu silicone rubber. The overall design is given in Figure 1.

OPEN ACCESS Freely available online
eISBN 978-967-0194-93-6 FBME

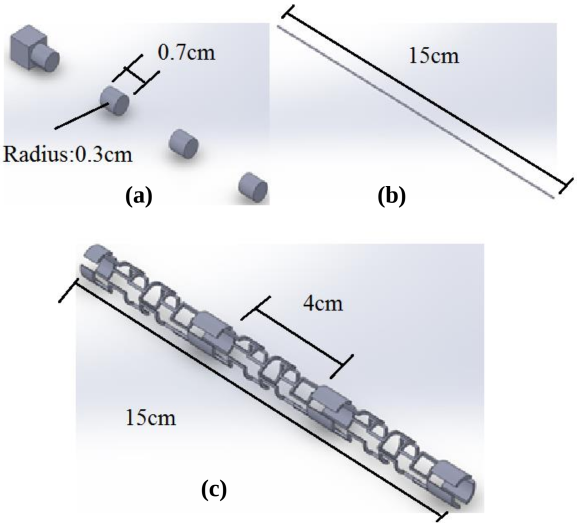

Fig. 1 Individual parts of the proposed instrument that consist of (a)spacer rings, (b)super-elastic backbone, (c)Nitinol actuator.

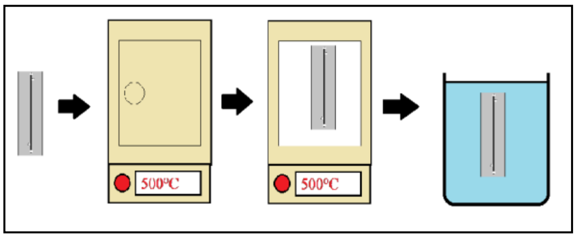

Fig. 2 Diagram of Shape Training Process.

Fig. 3 Furnace for training of Nitinol actuators.

Training of Shape Memory Alloy

Nitinol actuators required special heat treatment in order to "memorize" certain shapes. The Nitinol actuator could be changed into the shape as set using the mould by heating it. During this process, the actuator was set down into the aluminium mould to ensure that the shape did not deviate from the desired shape during the heating process. Once the Nitinol was set down on the mould, it was placed in a furnace which was pre-heated to 500°C for 15 minutes and then quenched in distilled water. The process was repeated 3 times to ensure that the shape training was effective. Figure 2 shows a simplified diagram of the shape training process. Figure 3 shows the furnace for the training process.

Fabrication of Spacer Rings

Once the design was made, the spacer rings of the instrument were then fabricated using a 3D printer. The 3D model created from Solidworks was used in this process. The material used Visijet® FTX Green which was solidified using a UV laser in a specific shape to produce the desired shape. The Nitinol actuators and tsuper-elastic alloy backbone were attached to the spacer rings using cyanoacrylic resin.

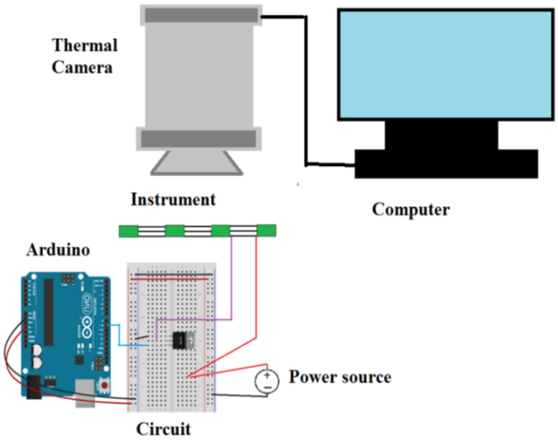

Fig. 4 Diagram of Thermal Current Test for instrument.

Fig. 5 Experimental setup for the Thermal Current Test with the usage of the thermal camera.

Fabrication of Silicone Rubber Sheathe

The silicone rubber sheathe was fabricated due to concerns that the Nitinol actuators heated up to above safe temperatures which was 42°C (Yarmolenko *et al.*, 2011).. The silicone rubber sheathe was made with two part Shin Etsu silicone rubber sheathe. The two parts were mixed with 1:1 weight ratio, then degassed with the vacuum pump to remove the air bubbles. The mixture was poured into a mould and cured to harden for 24 hours. Then, the sheathe was removed from the mould.

Thermal and Angle Current Test

The instrument was tested in terms of current to determine the most conducive current for the instrument. The produced current for the highest bending angle must not exceed the safe threshold temperature of 42°C. The tests were done using a PWM generator at a constant 70% duty cycle while varying the current from 0A until 1A. A thermal camera with a maximum of 45°C and a minimum detected temperature of 20°C was used to observe the temperature increment. Figure 4 illustrates the diagram for the experimental setup for the thermal current test. Figure 5 shows the actual experimental setup of the test.

Angle Current Test

The same experimental setup in the thermal current test was also used for the angle current test, but the thermal camera was replaced by a video camera. The current supply to the instrument was varied from 0A to 1A while undergoing a PWM signal with 70% duty cycle.

The video camera data was used to analyse the bending angle. These tests were done with and without the silicone rubber covering

OPEN ACCESS Freely available online
eISBN 978-967-0194-93-6 FBME

to see the difference in thermal characteristics of the instrument with and without the silicone rubber sheathe.

RESULTS AND DISCUSSION

Thermal Current Test

The thermal current results were analysed by dividing the analysis of the instrument to spacer ring A, spacer ring B and the actuator segment. Figure 6- 8 shows the plots of the thermal data for both covered and uncovered thermal current tests.

From the plots, we see that the addition of the silicone rubber sheathe raises the temperature of the instrument at the actuator area. This is due to the silicone rubber sheathe blocked the circulation air, thus trapping the hot air in the instrument causing a rise in actuator temperature.

On the spacer ring segment A and B, the temperature in spacer ring A for the test with the silicone rubber sheathe was much lower from 0mA until 700mA. However, the temperature readings are similar for the test on above 700mA. In spacer ring B, both tests show nearly the same results. This means that the silicone rubber sheathe is successfully able to lower the surface temperature of the instruments at the spacer rings but increase the temperature of the actuator segments for applications at 700mA.

We can also see that most of the heat was concentrated into the connection between the actuators and the wires. This means that the metallic crimping and cyanoacrylic used to bind the actuators and the wires were producing more heat than the actuators. Improvements need to be done to remedy this problem, including replacing these connections with a better connector, such as silver epoxy resin.

The tests also show that the instrument temperature is below 42°C for both tests, with and without the silicone rubber sheathe. This shows that the instrument is capable of bending without producing any damage to the surrounding tissues due to heat exposure.

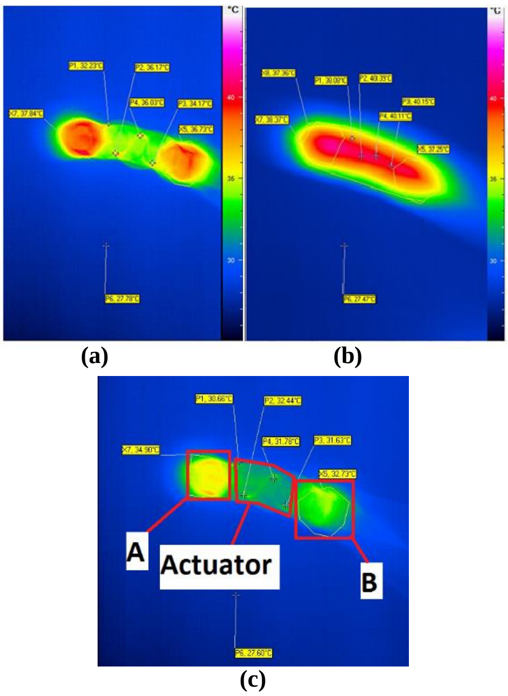

Fig. 6 Profile of thermal current test (a) uncovered instrument thermal current test (b) covered instrument thermal current test (c) analysis of thermal data by dividing into separate sections.

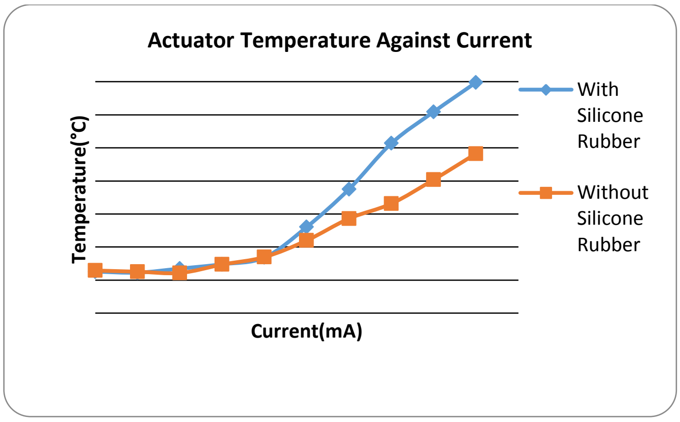

Fig. 6 Plot of temperature against current level for both covered and uncovered thermal test for the actuator segment

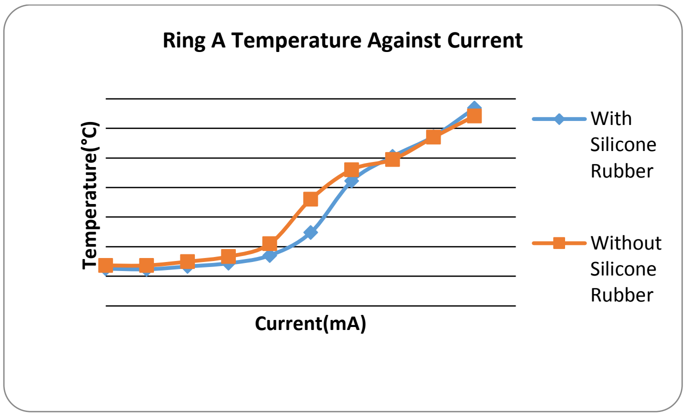

.

Fig. 7 Plot of temperature against current level for both covered and uncovered thermal test for the spacer rIng A segment

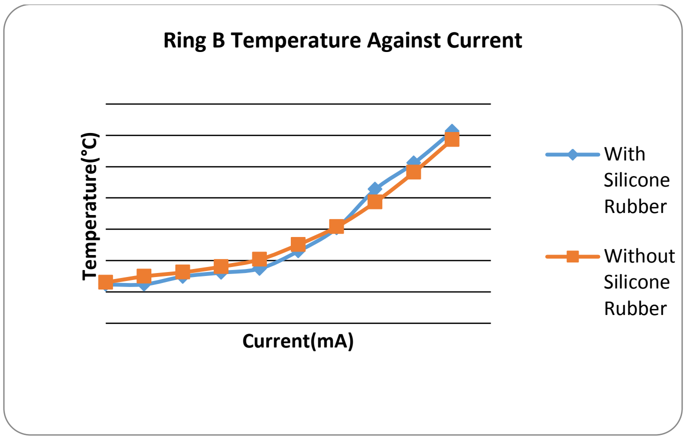

Fig. 8 Plot of temperature against current level for both covered and uncovered thermal test for the spacer rIng B segment

Angle Current Test

Images of the result analysis of the angle current test are shown in Figure 5. Image processing software was used to analyze the angle of bending of the instruments at different current intervals. The first blue line represents the initial angle, while the second blue line represents the angle after bending.

OPEN ACCESS Freely available online
eISBN 978-967-0194-93-6 FBME

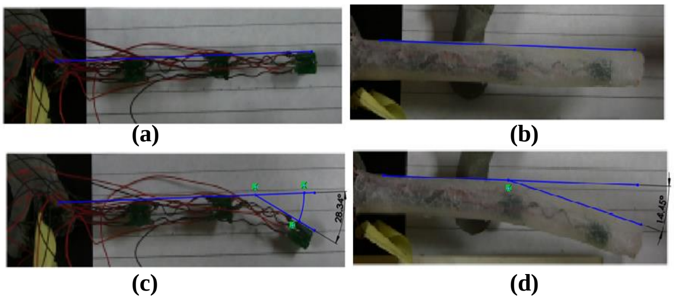

Fig. 9 Angle current tests of (a) initial uncovered instrument angle (b) initial covered instrument angle (c) bending uncovered instrument angle (d) bending covered instrument angle.

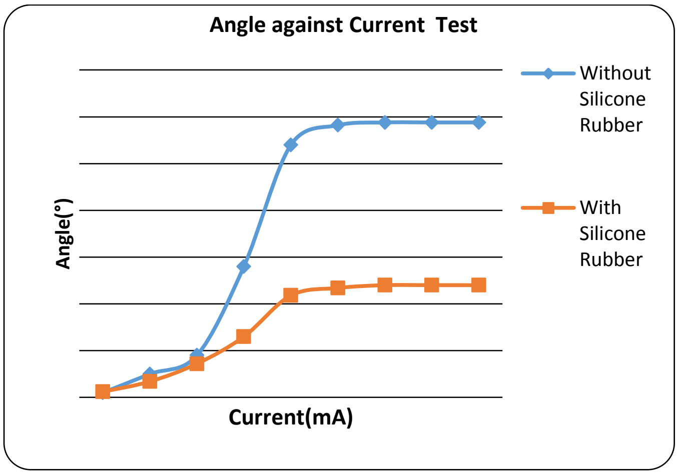

Fig. 10 Graph of angle of bending against current level for both covered and uncovered test.

The results show that maximum angle occurs when the current is raised until 700mA for both tests with and without the silicone rubber sheathe. This means that 700mA at 70% duty cycle is the optimum level of current to produce maximum amount of bending. Any further increase in current does not increase the bending angle.

We can also see that the bending angle for the test with the silicone cover produces a much lower angle of bending of only 12° compared to the angle of bending without the silicone rubber sheathe with a bending angle of 30°. This is due to the silicone rubber sheathe has certain material characteristics and thickness that add further resistance against the bending of the instrument due to its elasticity.

CONCLUSION

The instrument shows positive bending with the most suitable current used is 700mA DC power at 70% duty cycle. The maximum bending angle obtained is 30° for the uncovered instrument but only 12° for the instrument covered with the silicone rubber sheathe. The thermal test shows that the addition of the silicone rubber sheathe increases the temperature of the actuator segment but lowers the spacer ring temperature but both are still within safe ranges of temperatures. This shows that the addition of the silicone rubber sheathe does not improve the thermal characteristics of the instrument.

ACKNOWLEDGEMENT

This work was financially supported by the Universiti Teknologi Malaysia and Ministry of Higher Education of Malaysia grants underFRGS Grant R.J130000.7845.4F764 and AUNSEED Net Grant R.J130000.7323.4B187..

REFERENCES

Hansen, J. 2010. *Netter's Clinical Anatomy.* New York: Saunders.

Johannes Bodner, F. 2010. The da Vinci Robotic System for General Surgical Application: A Critical Interim Appraisal. *Swiss Medical Weekly*, 251-264.

Park, A. E. 2011. Evolution of Minimally Invasive Surgery and Its Impact on Surgical Residency Training . *Minimally Invasive Surgical Oncology*, 11-21.

Pavel S. Yarmolenko, E. J. 2011. Thresholds for Thermal Dmage to Normal Tissues: An update. *International Journal of Hyperthermia*, 320-343.

Sars, V. D. 2010. A Practical Approach to the Design and Control of Active Endoscope. *Mechatronics*, 251-264.

BIBLIOGRAPHY Axcrona, K., Berge, V. 2014. Review: Minimally Invasive Radical Prostatectomy - a Continuous Developement. *European Medical Journal*, 1-7.

Haga, Y., Mizushima, M., Matsunaga, T., Esashi, M. 2005. Medical and Welfare Applications of Shape Memory Alloy Microcoil Actuators. *Smart Materials and Structures*, 266-272.

Ho, M. M. 2011. Towards a Meso-Scale SMA-Actuated MRI-Compatible Neurosurgical Robot. *IEEE Transactions on Robotics : A Publication of the IEEE Robotics and Automation Society*, 1-10.

Zainal, M. A., Sahlan, S., & Ali, M. S. 2015. Micromachined shape-memory-alloy microactuators and their application in biomedical devices. *Micromachines*, 879-901.

AbuZaiter, A., Hikmat, O. F., Nafea, M., & Ali, M. S. M. (2016). Design and fabrication of a novel XYθz monolithic micro-positioning stage driven by NiTi shape-memory-alloy actuators. *Smart Materials and Structures*, *25*(10), [105004]. DOI: 10.1088/0964-1726/25/10/105004

OPEN ACCESS Freely available online
eISBN 978-967-0194-93-6 FBME